

Scaling laws verification for capacitive rf-discharge Ar plasma using particle-in-cell simulations

T. H. Chung^{a)} and H. S. Yoon

Department of Physics, Dong-A University, Pusan 604-714, Korea

J. K. Lee

Department of Physics, Pohang University of Science and Technology, Pohang 790-784, Korea

(Received 7 April 1995; accepted for publication 11 August 1995)

The characteristics of a 13.56 MHz capacitively coupled rf glow-discharge Ar plasma are studied by particle-in-cell simulation. The model simulates a planar plasma device which can be approximated using a one-dimensional plasma model. The model has proven to be useful to investigate the effect of varying control parameters such as neutral gas pressure, driver frequency, applied rf voltage on the characteristics of the discharge. A set of equations describing the dynamics of the system are presented and used to give analytic scaling laws. The simulation code is used to calculate the pressure dependence of plasma density, sheath width, peak position of the ionization event, and absorbed rf power. Scaling laws relating the control parameters to other operating functions such as average plasma potential, central electron density, absorbed rf power are examined and these functions are compared with simple analytical scaling formula. © 1995 American Institute of Physics.

I. INTRODUCTION

The role of plasma processing is becoming even more important with decreasing feature sizes on semiconductor wafers.¹ The characteristics of deposited materials and the rate of its generation are mainly dependent on the condition under which the plasma is generated. Understanding how and where plasma is created and identifying creation, loss, and transport mechanisms for various species in the plasma can assist in the design and production of more efficient plasma sources.

The commonly used reactor creates a discharge by radio frequency energy coupled to one electrode of a parallel plate system at pressures between 10^{-2} and 10 Torr.^{2,3} However, the capacitive rf sources suffer from the lack of independent control of ion flux and ion energy. In order to increase the plasma density, one raises the rf voltage, but this also raises the average plasma potential, increasing simultaneously the ion energy impacting the substrate.

Despite the extensive use of gas plasmas, the intricate nature of the gas discharge is poorly understood. This is mainly due to the complexity of the discharge. Electron processes include energy-dependent ionization, excitation, and elastic scattering; electron energy losses to the electrodes; electron ohmic heating in the sheaths and bulk plasma; stochastic heating by the oscillating electric fields in the sheath; secondary electron emission; and secondary electron-neutral ionization. Ion processes include ion energy losses to the electrode; ambipolar ion diffusion; ion acceleration in self-consistent sheaths; and production of secondary electrons.⁴ The secondary electron emission from the electrode surface by such ion bombardment plays an important role in sustaining the discharges. Discharges are used in pulsed-power devices, gas lasers, semiconductor etching, thin-film deposition, and plasma modification of materials.¹

There are several different approaches that can be taken in modeling rf discharges. The fluid simulations⁵⁻⁸ treat electrons and ions in the discharge as interpenetrating fluids immersed in neutral fluid. This approach assumes that the velocity distribution of the particles is Maxwell-Boltzmann distribution. Since in rf discharges the particle velocity distributions are not Maxwellian, there has been continuing effort to develop self-consistent kinetic models.⁹

A particle-in-cell (PIC) technique¹⁰⁻¹⁸ is an efficient and conceptually simple method of solving a wide variety of complex problems involving a large number of particles moving under the action of self-generated and externally imposed forces. In this study, weakly ionized processing plasmas are studied in one dimension using a bounded particle-in-cell simulation code with a Monte Carlo collision (PDP-1 code).¹⁴ We are considering a planar two-electrode rf discharge system which can be approximated using a one-dimensional plasma model.

This approach not only describes the basic dynamics of the discharge, but can be used as a tool to predict the correlations among different parameters of the discharge. Therefore, it is possible to do parametric studies using this approach. Given the control parameters p (neutral gas pressure), l (system length), V_{rf} (applied rf voltage), ω (driver frequency), and γ (secondary electron emission coefficient), the PDP-1 code^{12,14} has been used to obtain the time evolutions of T_e (electron temperature), n_o (plasma density), P_{rf} (rf power), J_i (ion current density to the electrode), J_{rf} (rf current density), s (sheath width), V_s (sheath potential).

Using the code, the dependence of the sheath width, the plasma density, the electron and ion energy distribution, the spatial distribution of the plasma density and potential on the control parameters are calculated and compared with other simulation results.^{19,20} The dependence of these functions on the applied rf voltage, V_{rf} , is also investigated.

^{a)}FAX: 82-51-200-7205; Electronic mail: thchung@seunghak.donga.ac.kr

II. SCALING LAWS OF THE CAPACITIVE rf DISCHARGE

Most of the complexity of rf discharge plasmas arises from the fact that many plasma parameters are interrelated. The state of a discharge is specified once a complete set of control parameters are given. The remaining plasma and equivalent circuit parameters are then specified as a function of the control parameters. Given the control parameters p, l, V_{rf}, ω , the models to determine $n_e, T_e, s, J_{rf}, P_{rf}$ have been developed.^{4,21,22} These models were based on simple approximations and needs to be verified to be valid for a broad range of experimental conditions. A self-consistent analytic solution for the dynamics of a high voltage capacitive rf sheath driven by a sinusoidal voltage source was obtained.²¹⁻²³

The electron sheath oscillates between a maximum thickness and a minimum thickness of a few Debye lengths from the electrode surface. The power is transferred to the charged particles in the discharge by rf fields in the sheaths and bulk plasma. The power gained by the sheath and bulk electrons through Ohmic heating (\bar{S}_{ohm}) and through stochastic heating (\bar{S}_{stoc}) by the oscillating sheath plasma boundaries is written as⁴

$$\bar{S}_{el} = \bar{S}_{stoc} + \bar{S}_{ohm}. \quad (1)$$

The stochastic heating and Ohmic heating scale as

$$\bar{S}_{stoc} \approx \left(\frac{m}{e}\right)^2 \epsilon_0 \omega^2 T_e^{1/2} V_1, \quad (2)$$

$$\bar{S}_{ohm} \approx 1.73 \frac{m}{2e} \epsilon_0 \omega^2 \nu_m T_e^{1/2} V_1 l, \quad (3)$$

where m is the electron mass, e is the electronic charge, ϵ_0 is the permittivity of vacuum, ν_m is the electron collision frequency with neutrals, l is the plasma length, T_e is the electron temperature, and V_1 is the fundamental rf voltage. \bar{S}_{el} must be equal to the power lost by collisions to the neutrals (\bar{S}_{coll}) and also by escape from the plasma to the electrode (\bar{S}_{esc})

$$\bar{S}_{el} = \bar{S}_{coll} + \bar{S}_{esc} \approx n_s u_B \epsilon_c, \quad (4)$$

where ϵ_c is the electron energy loss per ionization event, n_s is the electron density at sheath edge, and u_B is the Bohm velocity.

The rf supply provides power to the ions escaping the plasma, the secondary electrons being injected into plasma, and the thermal electrons in the plasma. The total power absorbed by the plasma is

$$S_{abs} = 2en_s u_B (\epsilon_i + \epsilon_c + 2T_e), \quad (5)$$

where ϵ_i is the ion kinetic energy which is almost equal to the average sheath potential, \bar{V} . Here the electron portion equates to \bar{S}_{el} of Eq. (1),

$$\bar{S}_{el} = 2en_s u_B (\epsilon_c + 2T_e). \quad (6)$$

Assume $\epsilon_c \gg T_e$ and that the stochastic heating term is dominant ($\bar{S}_{el} \approx \bar{S}_{stoc}$), then combining Eq. (2) and Eq. (6) gives

$$n_s \propto \frac{\omega^2 V_1}{\epsilon_c}. \quad (7)$$

For low sheath voltage, $\epsilon_i \ll \epsilon_c$

$$S_{abs} = 2en_s u_B \epsilon_c \propto \omega^2 T_e^{1/2} V_1. \quad (8)$$

For high sheath voltage, $\epsilon_i \gg \epsilon_c$

$$S_{abs} = 2en_s u_B \bar{V} \propto \frac{\omega^2 T_e^{1/2} V_1^2}{\epsilon_c}. \quad (9)$$

From the Child-Langmuir law,

$$s^2 \propto \frac{\bar{V}^{3/2}}{n_s u_B}. \quad (10)$$

\bar{V} is the average sheath potential which is the sum of a dc component and the average of an ac component ($V_{ac} \approx 0.32V_{rf}$). When the electron temperature is a little higher (e.g., 5 V), $\bar{V} \approx 0.45V_{rf}$.

Using Eqs. (1) and (4) we obtain¹⁷

$$s \propto \frac{\bar{V}^{1/2}}{\omega T_e^{1/4} \sqrt{K_{ohm} + K_{stoc} \bar{V}^{1/2}}}, \quad (11)$$

where we used $\bar{V} \propto V_1$, K_{ohm} , K_{stoc} are constants. At low pressures the Ohmic heating is small compared to the stochastic heating. Most of the Ohmic heating occurs at the plasma edge.

Simple scaling formulae for predicting the behavior of some plasma parameters are derived in Eqs. (8), (9), (11) and these are compared with simulation and experimental results, finding good agreements. We wish to obtain scaling laws that can estimate a wider set of plasma parameters, however, the various regimes have different coefficients in the scaling, and sometimes different scalings. Therefore, it should be noted that the scaling laws presented here are not universal, and are restricted to a specific parameter regime.

III. RESULTS AND DISCUSSIONS

The simulated device has an area of $0.001m^2$ electrodes separated by 5 cm and operated at 13.56 MHz. A blocking capacitance in the external circuit is chosen to be $C_b = 100$ pF. The applied rf voltage is held at 200 V, and the neutral gas pressure varies from 3 mTorr to 800 mTorr. The secondary electron emission coefficient due to ion bombardment to the electrode is arbitrarily chosen to be 0.2 throughout this simulation.

Figures 1 and 2 show the spatially averaged plasma density and the sheath width as a function of neutral gas pressure, respectively. As the neutral gas pressure increases, the plasma density increases as $p^{0.08}$ while the sheath width decreases as $s \propto p^{-0.32}$ in a low pressure region (60 - 200 mTorr), and $s \propto p^{-0.51}$ in a high pressure region (200 - 500 mTorr). The collisions between charged particles and neutrals modify the character of the discharge and sheath. Mutukura *et al.* investigated the pressure dependence of the

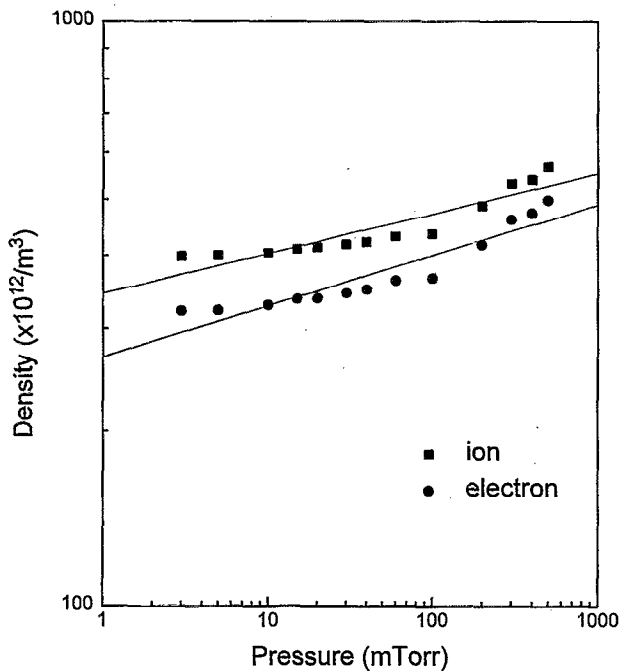


FIG. 1. Average plasma density as a function of gas pressure.

sheath thickness experimentally and analytically,²⁰ and their results are in agreement with the present simulation.

Figure 3 indicates the peak position of the ionization rate together with the sheath position at the driven electrode. The averaged ionization and excitation collision rates have relatively large values near both electrodes. Very near the electrode, the electron temperature is higher than in the bulk especially when the gas pressure is low, however, here the electron density is very low, resulting in very low ionization and excitation rates. A little distance away from the electrode, the average electron density becomes appreciable and

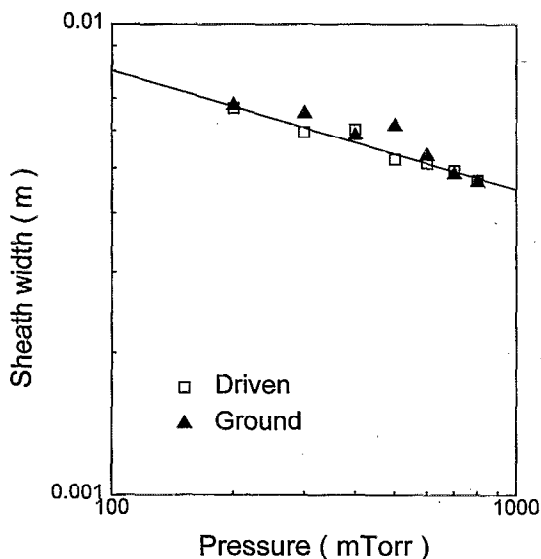


FIG. 2. Driven and grounded electrode sheath width as a function of gas pressure.

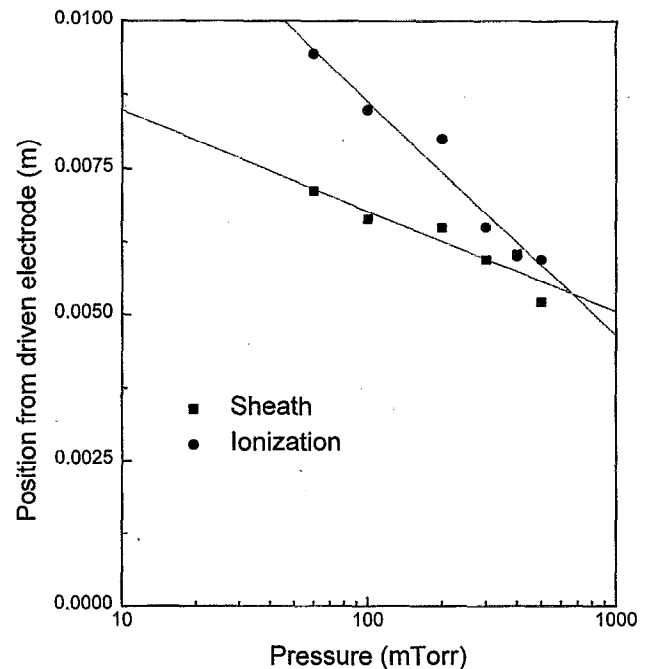


FIG. 3. The position from the driven electrode of the sheath and the ionization peak as a function of pressure. Here the gas pressure is 60 mTorr.

rate constants are still high. This results in high ionization and excitation rates around the plasma sheath edge. The points of maximum collision rate move closer to the electrodes as the pressure increases, and the sheath width shows the same behavior. The secondary and reflected electrons which are accelerated and heated in the sheath are responsible for the majority of the ionizing collisions and negative glows near the electrode. At intermediate pressures (150–400 mTorr) the dark space width agrees with the mean free path (also sheath width).²⁴

Figure 4 shows the calculation of the absorbed rf power P_{rf} vs p for two different values of applied rf voltage. Again, the variations of P_{rf} with p are in reasonable agreement with the analytic formula, Eqs. (1)–(4). Misium *et al.* showed that, at least at lower pressures, the dominant heating mechanism is a stochastic heating, that is, electron collisions with the oscillating sheath.⁴ In this work, the pressure range below 60 mTorr has not been explored, so the accurate scaling covering whole pressure range has not been obtained. However, at a low pressure region, the power scales as $\approx p^{0.5}$ which is different from Ohmic heating case (p^1) of Eq. (3). Therefore, we may state that the stochastic heating is dominant over the Ohmic heating. For $V_{rf}=200$ V, the power increases as $p^{0.45}$, and for $V_{rf}=500$ V, the power increases as $p^{0.65}$. This can be accounted for as the increasing portion of Ohmic heating with increasing V_{rf} . A similar scaling is found in the experimental results of Wood,²⁴ Godyak *et al.*,³ and the results typical in commercial etching reactors.²⁵

The power deposited into the system, the central electron density, the average plasma potential are plotted as a function of applied rf voltage in Figs. 5, 6, 7, respectively. In Fig. 5, we can note that the power scales as $V_{rf}^{1.5}$ which is between

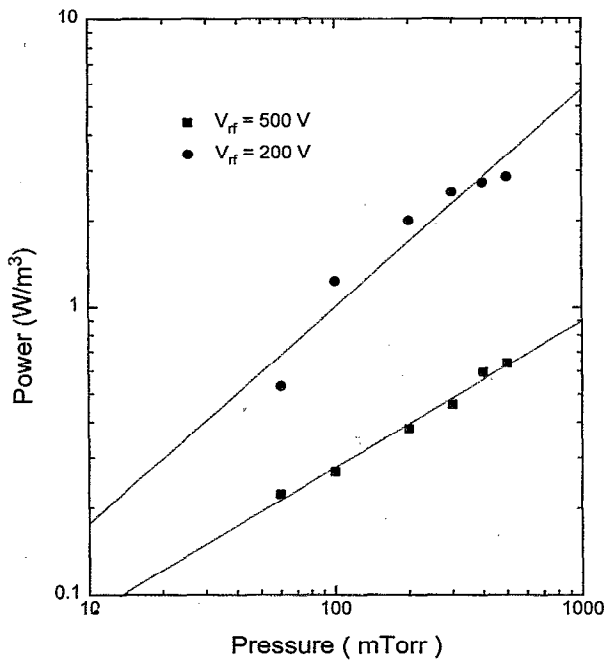


FIG. 4. Absorbed power vs pressure for two values of applied rf voltage.

V_{rf}^1 of Eq. (8) and V_{rf}^2 of Eq. (9). This indicates that the value of rf voltage used in this study is in the intermediate range between those of Eqs. (8) and (9). The experimental results of Wood also exhibit a similar scaling as $V_{rf}^{1.9}$.²⁴ In Fig. 6, the central electron density scales as $V_{rf}^{0.78}$ contrary to V_{rf}^1 of Eq. (7). The experimental results of Wood were $n_e \propto V_{rf}^{1.15}$ (at $p=30$ mTorr). In Fig. 7, the average plasma potential scales as $\approx 0.32V_{rf}$ because of a lower electron temperature than 5 V ($\bar{V} \approx 0.45V_{rf}$).²¹⁻²³

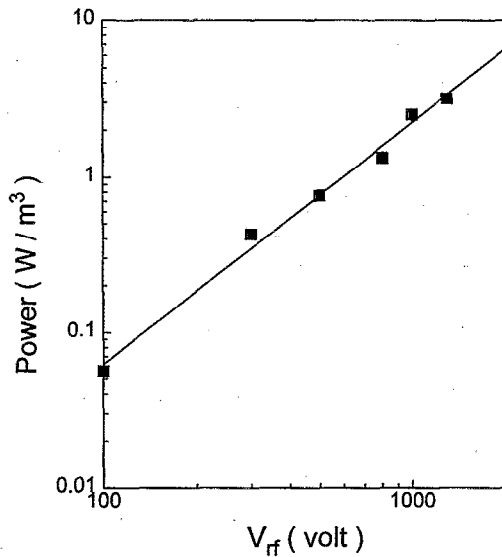


FIG. 5. Absorbed power vs applied rf voltage. Here the gas pressure is 60 mTorr.

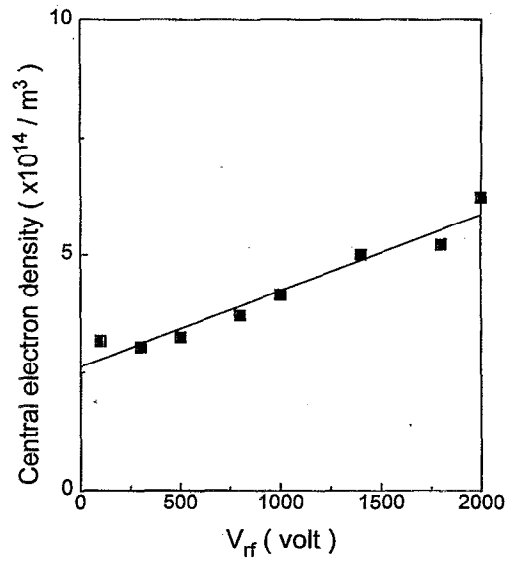


FIG. 6. Central electron density vs applied rf voltage. Here the gas pressure is 60 mTorr.

Figure 8 shows the rf power absorbed in the discharge as a function of driver frequency at a fixed pressure. The power scales as ω^2 which is in good agreement with Eqs. (8) and (9). As one can see in Fig. 9, the sheath width at the driven electrode is inversely proportional to the driver frequency as $\omega^{-0.2}$ contrary to Eq. (11), while in Fig. 10 the plasma density scales as $\omega^{0.5}$ contrary to Eq. (7). Equations (7) and (11) are based on a lot of assumptions and also depend on parameter regimes. The sheath width depends on applied rf volt-

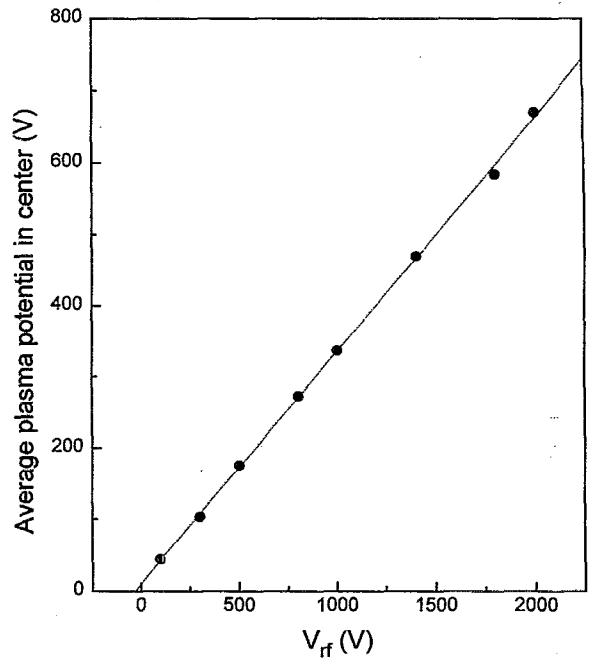


FIG. 7. Time-average plasma potential vs applied rf voltage. Here the gas pressure is 60 mTorr.

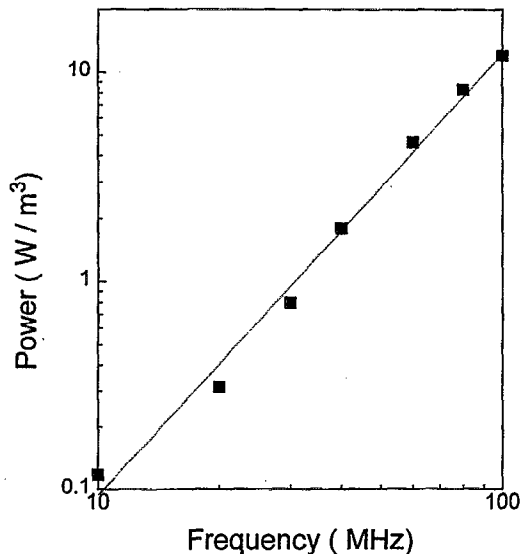


FIG. 8. Absorbed power vs driver frequency. Here the gas pressure is 60 mTorr.

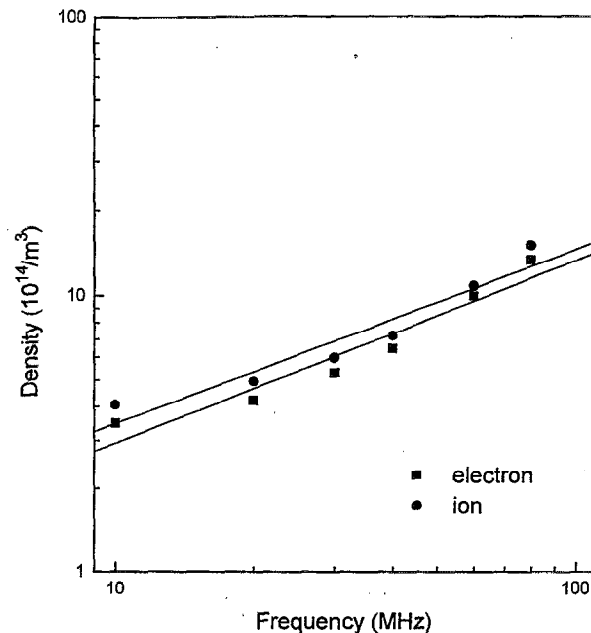


FIG. 10. Plasma density as a function of driver frequency. Here the gas pressure is 60 mTorr.

age, neutral pressure, plasma density, driver frequency, and electron temperature in a complicated way.^{21,22} Since these parameters are also interdependent, the sheath dependence on driver frequency is not simple. Those complexities can account for some discrepancies associated with the frequency dependence. To obtain the accurate and general scaling laws, the comparison between two-dimensional fluid simulation and PIC simulation is currently under development.²³

Figure 11 shows the sheath width as a function of applied rf voltage for two different values of gas pressure. For both cases the sheath scales as $V_{rf}^{0.25}$ which proves Eq. (11) in the stochastic heating dominant region. Experimental measurements in plasma discharge are sensitive to the specific equipment, configuration, and operation. Therefore one would not necessarily expect experiments to be directly com-

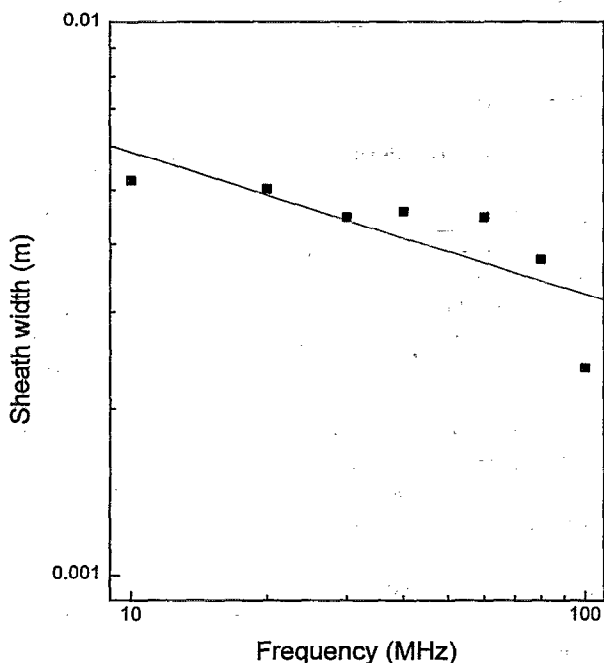


FIG. 9. Sheath width as a function of driver frequency. Here the gas pressure is 60 mTorr.

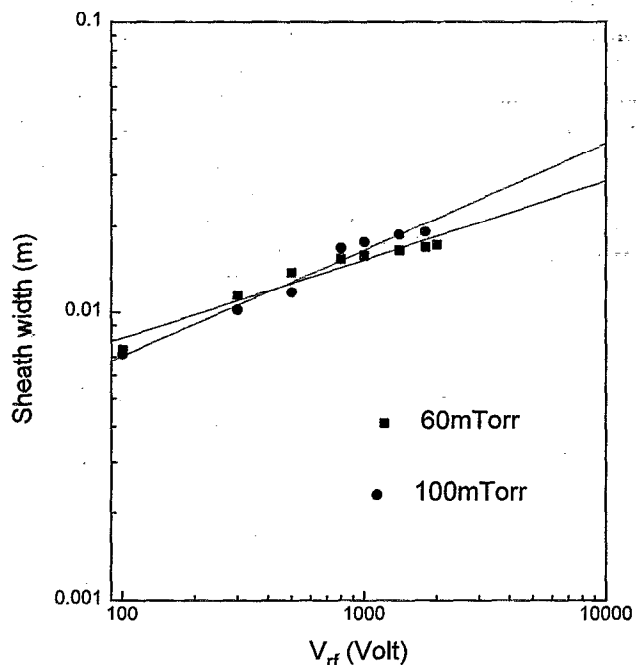


FIG. 11. Sheath width as a function of rf voltage for two different values of pressure.

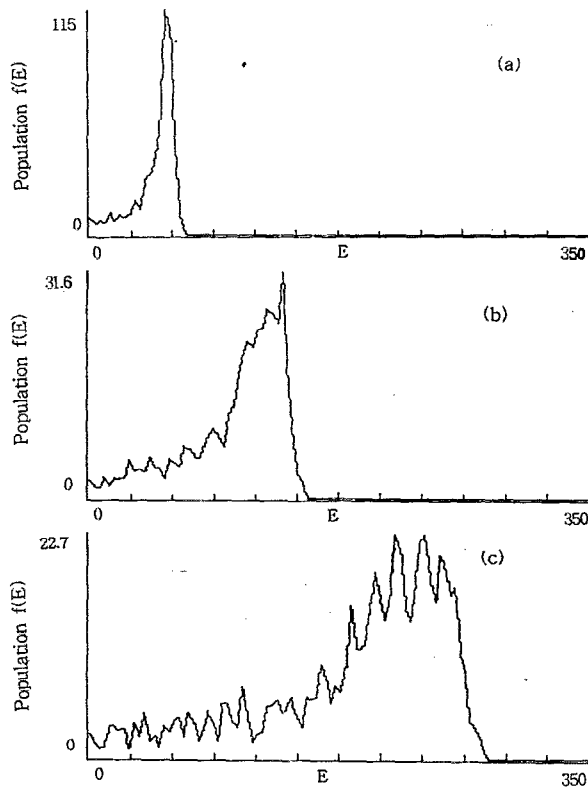


FIG. 12. Effect of rf voltage on the energy distribution of ions hitting to the electrode (a) $V_{rf}=100$ V, (b) 300 V, (c) 600 V. Here the gas pressure is 60 mTorr.

parable to analytic predictions and simulation results. But it is worthwhile to obtain scaling laws using simulation to compare to the analytic predictions and experimental results.

Ions entering the sheath from the plasma are accelerated when they cross the driven electrode sheath. Arriving at the driven electrode, ions have acquired a kinetic energy of the sheath potential difference, which is the sum of the average plasma potential and the dc bias voltage, and hit driven electrode. In collisionless sheaths, the crucial parameter determining the ion energy distribution is τ_{ion}/τ_{rf} (τ_{ion} is the ion transit time through the sheath and τ_{rf} is the rf period). If we assume a collisionless Child-Langmuir sheath,²⁹

$$\frac{\tau_{ion}}{\tau_{rf}} = \frac{3s\omega}{2\pi} \left(\frac{M}{2\pi\bar{V}} \right)^{1/2}, \quad (12)$$

where M is the ion mass. Figures 12 and 13 show the effect of applied rf voltage and driver frequency on the energy distribution of ions hitting the driven electrode, respectively. We can observe in Fig. 12 that as the applied rf voltage increases the high energy portion of the ion energy distribution increases. As the driver frequency is raised, τ_{ion}/τ_{rf} increases and then ions take many cycles to cross sheath and can only respond to average sheath voltage, and the two peaks of the ion energy distribution approach each other. But in Figs. 13(a) and 13(b), the second peak in bimodal shape energy distribution are not shown since those are too small.²⁹ In Fig. 13, it is seen that as the driver frequency increases the

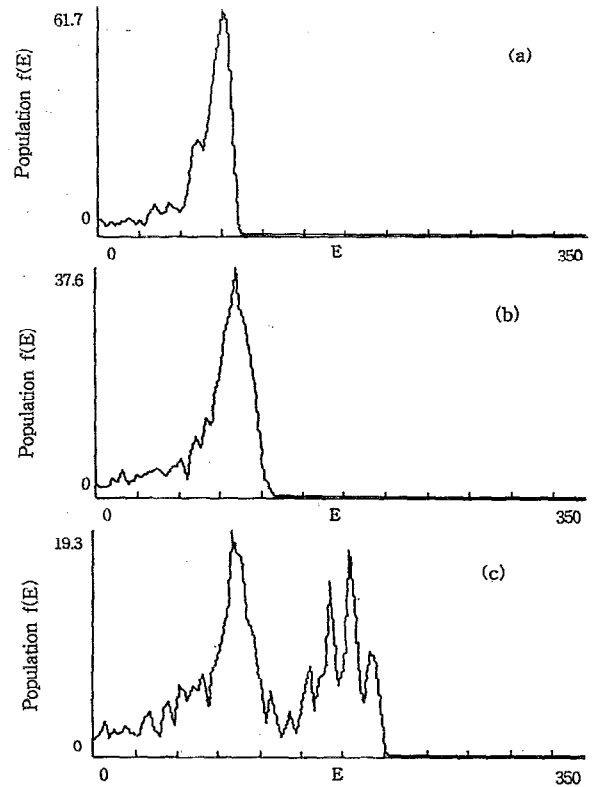


FIG. 13. Effect of driver frequency on the energy distribution of ions hitting to the electrode (a) 10 MHz, (b) 20 MHz, (c) 40 MHz. Here the gas pressure is 60 mTorr.

high energy portion of the ion energy distribution increases. This can be explained as the increase of driver frequency reduces collisions between ions and neutrals, thus resulting in higher ion energy. These results agree well with many experimental and simulation results.^{26,27}

IV. CONCLUSIONS

The characteristics of a 13.56 MHz capacitively coupled rf glow-discharge Ar plasma are studied by particle-in-cell simulation. The model simulates a planar plasma device and calculates the effect of varying control parameters such as neutral gas pressure, driver frequency, applied rf voltage on the characteristics of the discharge. The pressure dependences of plasma density, sheath width, peak position of the ionization event, and absorbed rf power are investigated. Scaling laws relating driver frequency and applied rf voltage to other operating functions such as plasma potential, central electron density, absorbed rf power are examined with numerical simulation and compared with simple analytical scaling formulae. Cases of various applied rf voltages and driver frequencies are shown. The simulation results are generally in good agreement with analytic scaling formulae. There are some discrepancies between the analytic predictions and simulation results. The reason for this is not clear at this point but is probably due to more complicated nature such as three-dimensional effect which has not been included in the one-dimensional PIC simulation scheme. However, the re-

sults of this study show that a PIC simulation can capture many main features predicted by the analytic model. The results can provide a useful tool for the design and analysis of plasma reactors.

ACKNOWLEDGMENTS

This work was supported in part by Korea Science and Engineering Foundation and Korea Ministry of Education (Basic Science Research Institute).

- ¹D.B. Graves, *IEEE Trans. Plasma Sci.* **22**, 31 (1994).
- ²V.A. Godyak and R.B. Piejak, *Phys. Rev. Lett.* **65**, 996 (1990).
- ³V.A. Godyak, R.B. Piejak, and B.M. Alexandrovich, *IEEE Trans. Plasma Sci.* **19**, 660 (1991).
- ⁴G.R. Misium, A.J. Lichtenberg, and M.A. Lieberman, *J. Vac. Sci. Technol. A* **7**, 1007 (1989).
- ⁵D.B. Graves, *J. Appl. Phys.* **62**, 88 (1987).
- ⁶D.B. Graves and K.F. Jensen, *IEEE Trans. Plasma Sci.* **14**, 78 (1986).
- ⁷S.K. Park and D.J. Economou, *J. Appl. Phys.* **68**, 3904 (1990).
- ⁸S.K. Park and D.J. Economou, *J. Appl. Phys.* **68**, 4888 (1990).
- ⁹T.J. Sommerer, W.N.G. Hitchon, R.E.P. Harvey, and J.E. Lawler, *Phys. Rev. A* **43**, 4452 (1991).
- ¹⁰W.S. Lawson, *J. Comput. Phys.* **80**, 253 (1989).
- ¹¹V. Vahedi, M.A. Lieberman, M.V. Alves, J.P. Verboncoeur, and C.K. Birdsall, *J. Appl. Phys.* **69**, 2008 (1991).
- ¹²M.V. Alves, M.A. Lieberman, V. Vahedi, and C.K. Birdsall, *J. Appl. Phys.* **69**, 3823 (1991).
- ¹³D. Vender and R.W. Boswell, *IEEE Trans. Plasma Sci.* **18**, 725 (1990).
- ¹⁴C.K. Birdsall, *IEEE Trans. Plasma Sci.* **19**, 65 (1991).
- ¹⁵M. Surendra, D.B. Graves, and I.J. Morey, *Appl. Phys. Lett.* **56**, 1022 (1990).
- ¹⁶M. Surendra and D.B. Graves, *IEEE Trans. Plasma Sci.* **19**, 144 (1991).
- ¹⁷V. Vahedi, C.K. Birdsall, M.A. Lieberman, G. Dipeso, and T.D. Rognlien, *Phys. Fluids B* **5**, 2719 (1993).
- ¹⁸S.C. Paek, S.R. Yoon, and Y.S. Cho, *J. Korean Phys. Soc.* **20**, 466 (1993).
- ¹⁹M. Surendra and D.B. Graves, *Appl. Phys. Lett.* **59**, 2091 (1991).
- ²⁰N. Mutsukura, K. Kobayashi, and Y. Machi, *J. Appl. Phys.* **68**, 2657 (1990).
- ²¹M.A. Lieberman, *IEEE Trans. Plasma Sci.* **16**, 638 (1988).
- ²²M.A. Lieberman, *IEEE Trans. Plasma Sci.* **17**, 338 (1989).
- ²³R.W. Boswell and I.J. Morey, *Appl. Phys. Lett.* **52**, 21 (1988).
- ²⁴B.P. Wood, Ph.D thesis, University of California at Berkeley, 1991.
- ²⁵J.W. Coburn and H.F. Winters, *Annu. Rev. Mater. Sci.* **13**, 91 (1983).
- ²⁶Ch. Wild and P. Koidl, *Appl. Phys. Lett.* **54**, 505 (1989).
- ²⁷J. Liu, G.L. Huppert, and H.H. Sawin, *J. Appl. Phys.* **68**, 3916 (1990).
- ²⁸T.H. Chung, H.J. Yoon, S.H. Lee, and J.K. Lee, to be presented at 37th Annual Meeting of APS Division of Plasma Physics, November 6-10, 1995.
- ²⁹E. Kawamura, V. Vahedi, M.A. Lieberman, and C.K. Birdsall, *Proceedings of the IEEE International Conference on Plasma Science*, Madison, WI, June 5-8 (IEEE, New York, 1995).